http://dx.doi.org/10.5012/bkcs.2014.35.3.938

Coherence Gated Three-dimensional Imaging System using Organic Photorefractive Holography†

Ui-Jung Hwang,[‡,a] Jongwan Choi,[‡,a] Chuntae Kim,[§] Won-Guen Kim,[§] Jin-Woo Oh,[§,*] and Nakjoong Kim[‡,*]

[‡]*Department of Chemistry and Research Institute for Natural Science, Hanyang University, Seoul 133-791, Korea*
[*]*E-mail: kimnj@hanyang.ac.kr*
[§]*Department of Nanofusion Technology and Department of Nanomaterials engineering, Pusan National University, Busan 609-735, Korea.* [*]*E-mail: ojw@pusan.ac.kr*
Received December 10, 2013, Accepted January 6, 2014

This paper discusses a coherence-gated three-dimensional imaging system based on photorefractive holography, which was applied to imaging through turbid media with a view to developing biomedical instrumentation. A rapid response photorefractive device doped with 2,4,7-trinitro-9-fluorenylidene malononitrile was used to generate the hologram grating. The estimated depth resolution was 20 μm, which corresponds to the coherence length of the light source. In this coherence imaging system, tomographic imaging of a 3-dimensional object composed of a 50 μm thick cylindrical layer was achieved. The proposed coherence imaging system using an organic photorefractive material can be used as an optical tomography system for biological applications

Key Words : 3D imaging system, Organic photorefractive material, Holography

Introduction

Several coherent imaging methods that function through scattering media by extracting unscattered ballistic light from a diffuse scattered background,[1,2] such as optical coherence tomography (OCT),[3] heterodyne detection,[4] and electronic[5] and photorefractive holography,[6,7] have been reported. Specifically, three-dimensional images are constructed by axially scanning the interferometer path difference between the object and the reference beams. OCT combines coherence gating with confocal imaging to provide a further rejection of scattered light.[8] Typically, OCT scans the sample axially, and further transverse scanning is needed to produce a 2D slice. Hence, it is not a real-time wide-field technique, even though it can provide 2D images at a reasonable frame rate.[9] Another drawback to OCT systems is the requirement for spatially coherent broadband radiation, which typically requires expensive, mode-locked Ti:sapphire lasers, or super luminescent diodes (SLD) that are limited in power to a few milliwatts.

Over the last few decades, a photorefractive (PR) effect has been observed with a variety of potential applications in holographic data storage and information processes, such as pattern recognition, phase conjugation mirrors, and optically-controlled spatial light modulators.[10,11] The photorefractive PR effect can also be used in the biomedical application of optical coherent tomography of thick biological tissues by recording the interferogram.[12] The advantage of PR materials is that they respond to the spatial derivative of a spatially modulated light field,[13,14] and not to the absolute light intensity, as is the case with most integrating detectors, such as CCDs or photographic emulsion.[8] In particular, the PR effect-based holographic method can achieve one full field image at a time without scanning. This paper reports coherence tomographic imaging using an organic photorefractive PR composite based holographic technique. A 2,4,7-trinitro-9-fluorenylidene malononitrile (TNFM)-sensitized, carbazole-based PR polymer with a rapid grating formation time was used for this application.

Experimental

Sample Preparation. The photoconducting polymer, poly[methyl-3-(9-carbazolyl)propylsiloxane] (PSX-Cz), and the nonlinear optical chromophore, 2-{3-[(*E*)-2-(dibutylamino)-1-ethenyl]-5,5-dimethyl-2-cyclohexenyliden} malononitrile (DB-IP-DC), were synthesized using a methodology reported elsewhere.[15,16] TNFM was purchased from Kanto Chemistry Co. and used after purification by vacuum sublimation. Figure 1 shows the chemical structures of the materials used in this study. Their chemical and physical properties are reported elsewhere.[17] A blended mixture of

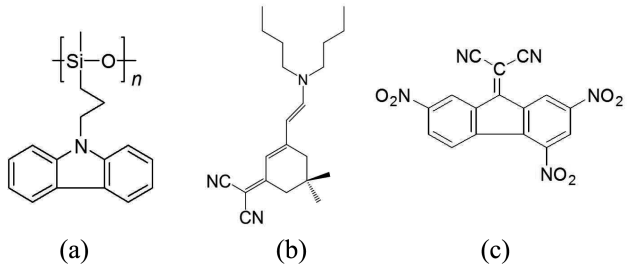

Figure 1. The chemical structure of the components in the organic PR composite: (a) PSX-Cz, (b) DB-IP-DC, (c) TNFM.

[a]These authors contributed equally to this work.
†This paper is to commemorate Professor Myung Soo Kim's honourable retirement.

PSX-Cz (69 wt %), DB-IP-DC (30 wt %), and TNFM (1 wt %) was dissolved in 1,2-dichlorobenzene for the PR composite. The resulting solution was drop-casted onto indium tin oxide (ITO) glass plates through a 0.2 μm PTFE filter. The sample was dried in an oven at 90 °C for 24 h to remove any residual solvent. The sample was then covered with a second ITO-coated glass. The film thickness was controlled using a 100 μm Teflon spacer between the two ITO glass plates.

Optic Configuration. Figure 2 shows the experimental setup used for the depth-resolved imaging. Light with a power of 12 mW from a SLD (830 nm) was divided using a beam splitter. The coherence length of the light source was estimated to be 20 μm by monitoring the interference pattern from a Michelson interferometer. The transmitted beam was reflected at the U.S. Air Force (USAF) test chart, which is coated with aluminum on the front surface and is composed of 1.6 mm thick glass. This signal beam images the sample plane using the lens with a focal length of 10 cm. The 3-dimensional test object for the depth sectioning experiment was composed of concentric cylinders, whose diameters are 1 mm, 2 mm, 3 mm, and 4 mm, respectively. Each cylinder height was approximately the same at 50 μm. The beam reflected from the beam splitter acted as a reference beam reflected on a mirror mounted on a micrometer-controlled x-translating stage. The reference beam traveled by reflecting from a few mirrors to satisfy the intended writing angle and optical path length. The bisector angle between the reference and the signal beam was 4.3, and the sample normal was tilted 45° from the bisector of the two writing beams. A pseudo image at the sample plane was imaged again on a CCD camera using an imaging lens with a focal length of 10 cm. To prevent the walk-off problem, a couple of prisms were inserted on the path of the reference arm instead of each prism at the reference and signal arm. Two prisms were identical and the uncoated right angle prism had a refractive index of 1.519 at 830 nm. Because the reference beam passes the prism four times, it is believed that the energy planes of the reference beam became parallel to the signal beam to enlarge the interfering area at the sample plain. After being recorded in a photorefractive composite device, the image was reproduced by blocking the signal beam. At this reading, the reference beam itself acted as the probing beam to diffract the recorded image. The image can be read with a third laser for a probe beam whose wavelength was the same as the writing beam. In this manner, real time recording and reading can be achieved. For the present material, the photo sensitivity decreases with a wavelength from approximately 600 nm to a longer one, as verified by UV-vis spectroscopy. Therefore, a laser beam with a wavelength of 830 nm or shorter for probing can erase a hologram recorded on a photorefractive medium, which can reduce the reconstructed image quality. A probing laser beam at wavelengths longer than 830 nm is preferred, but was not attempted in this stage.

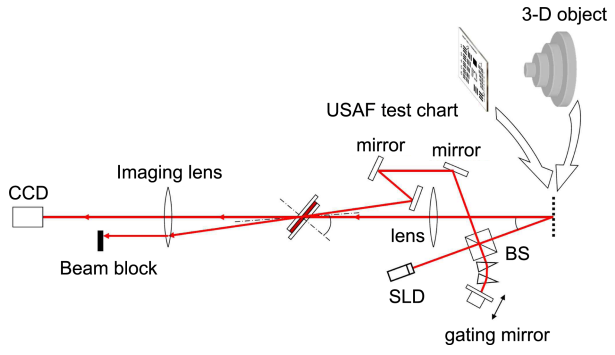

Figure 2. Experimental set up for achieving coherence imaging.

Results and Discussion

A TNFM-doped organic PR device was used to obtain rapid responsive coherence imaging. The increase in the absorption coefficient due to the high electron affinity of TNFM led to larger photoconductivity, a space charge field and rapid grating build-up through fast photo-charge generation.[18] Figure 3(a) shows an image of the test chart imaged directly by the CCD camera through a photorefractive device. Element 5 and 6 bars of group 1 with widths of 0.16 and 0.14 mm, respectively, were observed. Figure 3(b) represents a background image when the signal beam was blocked. This background was subtracted from the other images before being presented. Figures 3(c) to 3(g) show the reconstructed images and each image was recorded when the reference arm mirror was shifted in 10 μm steps. The depth resolution of this coherence imaging system was estimated to be 20 μm because the image of a surface was reconstructed in the range of the 20 μm reference arm position.

Another image was recorded on the composite at a point, 2.39 mm from the Figure 3(e). The image intensity was dimmed considerably but it was clear that the brightness and darkness of the image was reversed (Figure 3(e)). This image originates from the back side of the chart. The light reflected from the back side of the USAF test chart produced a hologram on the photorefractive device and the a back side image was reconstructed. The optical path length of the 1.6

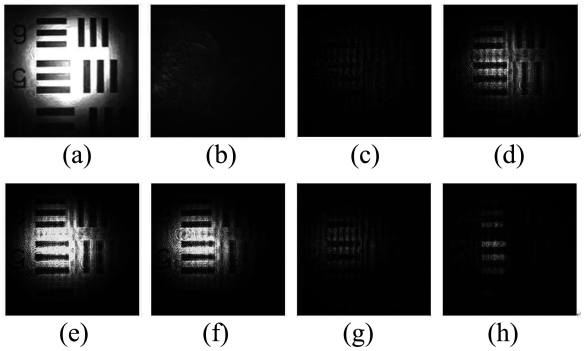

Figure 3. Reconstructed images of the USAF test chart. (a) original image of the chart, (b) background image, and (c)-(h) coherence gated images subtracted by image (b). The position of the reference arm was shifted by 10 micron for each image except image (h). The reference arm position for image (e) and (h) differs by 2.39 mm.

Figure 4. Reconstructed images of a 3-dimensional object composed of some cylindrical layers with different diameters. (a) original image of the object, (b) background image, and (c)-(e) coherence gated images subtracted by image (b). The position of the reference arm was shifted by 10 micron for each image.

mm thick test chart was approximately 2.43 mm, considering the index of the material. The optical path length showed good agreement with a gating mirror distance of 2.39 mm.

A 3-dimensional test object was placed instead of the USAF test chart to clarify the tomographic ability of this system. Figure 4(a) presents a rare image of the test object through a photorefractive device. The surfaces of the top 3 cylindrical layers of the object were partially observed in the image. Figures 4(c) to 4(e) present the coherence gated reconstructed images with the background subtracted, as shown in Figure 4(b). For each sectioned image, the reference arm mirror was shifted in 40 μm steps. As shown in Figure 4, tomographic images of a 3-dimensional object were successfully achieved. A lathe manufactured, 50 μm high cylinder was depicted as a 40 μm high cylinder using this coherence gate imaging system. These results are quite reasonable considering that the error range of the lathe used to cut the 3-dimensional object was 10 μm.

Conclusion

Coherence tomographic imaging was demonstrated by a holographic technique using an organic photorefractive composite. The depth resolution was estimated to be 20 μm, which corresponds to the coherence length of the light source (super luminescent diode) used in this study. In this coherence imaging system, tomographic imaging of a 3-dimensional object composed of a 50 μm thick cylindrical layer was achieved. This suggests that coherence imaging using a photorefractive polymer material is a promising optical tomography system for use in biological applications.

Acknowledgments. This work was supported by the National Research Foundation (NRF) grant funded by the Korea government (MSIP) through the Active Polymer Center for Pattern Integration (No. 2007-0056091) and the 2012 Specialization Project Research Grant funded by the Pusan National University.

References

1. Stetson, K. A. *J. Opt. Soc. Am.* **1967**, *57*, 1060.
2. Caulfield, H. J. *J. Opt. Soc. Am.* **1968**, *58*, 276.
3. Huang, D.; Swanson, E. A.; Li, P.; Schuman, J. S.; Stinson, W. G.; Chang, W.; Hee, M. R.; Flotte, T.; Gregory, K.; Puliato, C. A.; Fujimoto, J. G. *Science* **1991**, *254*, 1178.
4. Chan, K. P.; Yamada, M.; Inaba, H. *Electron. Lett.* **1994**, *30*, 17535.
5. Chen, H.; Chen, Y.; Dilworth, D.; Leith, E. N.; Lopez, J.; Valdmanis, J. *Opt. Lett.* **1991**, *16*, 487.
6. Rebane, A.; Feinberg, J. *Nature* **1991**, *331*, 378.
7. Hyde, S. C. W.; Jones, R.; Barry, N. P.; Dainty, J. C.; French, P. M. W.; Kwolek, K. M.; Nolte, D. D.; Melloch, M. R. *IEEE J. Select. Top. Quantum Electron.* **1996**, *2*, 965.
8. Gu, Y.; Ansari, Z.; Dunsby, C.; Parsons-Karavassilis, D.; Siegel, J.; Itoh, M.; French, P. M. W.; Nolte, D. D.; Headley, W.; Melloch, M. R. *J. Mod. Optic*. **2002**, *49*, 877.
9. Rollins, A. M.; Kulkarni, M. D.; Yazdanfar, S.; Ung-arunyawee, R.; Izatt, J. A. *Opt. Express* **1998**, *3*, 219.
10. Kamshilin, A. A.; Liu, S.; Tuovinen, H.; Prokofiev, V. V.; Jaaskelainen, T. *Opt. Lett*. **1994**, *19*, 907.
11. Oh, J.-W.; Joo, W.-J.; Moon, I.-K.; Choi, C.-S.; Kim, N. *J. Phys. Chem. B* **2009**, *113*, 1592.
12. Yu, P.; Balasubramanian, S.; Ward, T. Z.; Chandrasekhar, M.; Chandrasekhar, H. R. *Synth. Met*. **2005**, *155*, 406.
13. Günther, P., Huignard, J. P., Eds.; *Photorefractive Materials and Their Applications I and II*; Springer-Verlag: Berlin Heidelberg, Germany, 1988.
14. Oh, J.-W.; Choi, C.-S.; Jung, Y.; Lee, C.; Kim, N. *J. Mater. Chem*. **2009**, *19*, 5765.
15. Chun, H.; Moon, I. K.; Shin, D.-H.; Kim, N. *Chem. Meter*. **2001**, *13*, 2813.
16. Oh, J.-W.; Lee, C; Kim, N. *J. Chem. Phys*. **2009**, *130*, 134909.
17. Oh, J.-W.; Choi, J.; Kim, N. *Macromol. Res*. **2009**, *17*, 69.
18. Oh, J.-W.; Kim, N. *J. Photoch. Photobio. A* **2009**, *201*, 222.